EDGE ARTICLE

Check for updates

Light-initiated 1,3-dipolar cycloaddition between dehydroalanines and tetrazoles: application to late-stage peptide and protein modifications†

Mengqian Zhang, [ID] [a] Peiyang He [ID] [a] and Yanmei Li [ID] *[abc]

As an easily introduced noncoded amino acid with unique electrophilicity distinct from the 20 natural amino acids, dehydroalanine (Dha) is not only a precise protein post-translational modification (PTM) insertion tool, but also a promising multifunctional labelling site for peptides and proteins. However, achieving a balance between the reaction rate and mild reaction conditions has been a major challenge in developing novel Dha-modified strategies. Rapid, efficient, and mild Dha modification strategies are highly desired. Additionally, catalyst-free photocontrollable reactions for Dha-containing peptide and protein modification have yet to be developed. Here, we report a photoinitiated 1,3-dipolar cycloaddition reaction between Dha and 2,5-diaryl tetrazoles. Under low-power UV lamp irradiation, this reaction is completed within minutes without catalysis, resulting in a fluorescent pyrazoline-modified peptide or protein with excellent chemoselectivity for Dha residues. Notably, this reaction exhibits complete site-specificity in the modification of thiostrepton, a natural antimicrobial peptide containing multiple Dha residues (Dha3, Dha16, and Dha17), within 20 minutes in high yields. This is currently the fastest reaction for modifying the Dha residue in thiostrepton with clear site-specificity towards Dha16. This photoinitiated reaction also provides a chemoselective strategy for precise functionalization of proteins. Additionally, the rapidity and efficiency of the reaction minimize UV light damage to the biological reaction system. Combined with fluorogenic properties, this photo-controllable methodology can be applied to live cell imaging, further broadening the application scope of the Dha modification methodology.

Introduction

Chemical modifications provide basic tools for conferring, regulating or improving peptide and protein functions in biology and medicine. As a result, this toolbox has a wide range of applications in peptide and protein science, including but not limited to post-translational modification (PTM) insertion, fluorescence tracking and targeted delivery.[1–3] To date, various chemoselective modification strategies have been developed. However, strategies targeting specific canonical amino acids in peptides and proteins tend to generate multisite modification products.[4,5] To achieve more precise site-selective modification, methods targeting noncoded amino acids with unique reactivity need to be further developed.[1]

Dehydroalanine (Dha) has been an attractive option for precise late-stage modification of peptides and proteins. As a naturally occurring noncoded amino acid,[6] it is formed by serine (Ser) dehydration or phosphoserine (pSer) elimination in natural peptides[7–9] and proteins.[10,11] In particular, employing cysteine (Cys) and serine (Ser) as precursors, Dha can be easily introduced into various peptides and proteins at the position of interest *via* mild chemical treatment.[10,12] In addition, owing to its electrophilic α,β-unsaturated structure, Dha has a unique chemical reactivity distinct from the 20 natural amino acids, which facilitates site-selective modification of peptides and proteins. To date, various robust Dha modification strategies have been reported, such as nucleophilic additions for the construction of carbon–heteroatomic (C–X) bonds and radical additions or metal-catalysed cross-coupling reactions for the formation of carbon–carbon (C–C) bonds on the β-C of Dha residues (Fig. 1).[13,14] These reactions have been applied in protein therapeutics, such as the preparation of homologous antibody–drug conjugates (ADCs),[15] as well as the insertion of PTMs and their mimics, to explore the influence on protein structures and functions.[16,17] In addition, the cycloaddition reaction has been another approach to Dha modification, yet it is still only in its infancy. To date, related strategies have mainly

[a]Key Laboratory of Bioorganic Phosphorus Chemistry and Chemical Biology, Department of Chemistry, Tsinghua University, Beijing 100084, P. R. China. E-mail: liym@mail.tsinghua.edu.cn

[b]Beijing Institute for Brain Disorders, Beijing 100069, P. R. China

[c]Center for Synthetic and Systems Biology, Tsinghua University, Beijing 100084, P. R. China

† Electronic supplementary information (ESI) available. See DOI: https://doi.org/10.1039/d3sc02818f

Fig. 1 Strategies for Dha-containing peptide and protein modification. [a]Only one cycloaddition strategy for protein modification has been reported so far.

focused on the modification of small molecule Dha derivatives and peptides.[18–20]

Despite these advances, there is still much room for the development and improvement of Dha chemistry. First, the competing electronic forces between the π-donating nitrogen substituent and electron-withdrawing carbonyl group reduce the reactivity of Dha to some extent.[10,18] As a result, most peptide or protein Dha modification reactions require hours to days to complete (Fig. 1A).[13] For instance, nucleophilic addition reactions typically take 1 to 12 hours[15,21–25] to form C–X bonds. Free radical reactions, on the other hand, usually take 0.5 to 24 hours to complete,[17,26–32] with only a small proportion of reactions[17,29] finishing within an hour. Cycloaddition reactions need even longer reaction times, varying from 2 to 72 hours.[18–20,33] Therefore, more rapid and efficient Dha modification strategies are highly desired. In addition, Dha modification reactions developed in recent years are generally not mild enough, requiring the use of organic solvents and/or harsh catalysts, causing difficulty in further biomedical applications. Hence, non-catalytic and mild bioorthogonal Dha modification reactions remain to be developed. Last, previously developed strategies focused more on introducing specific amino acids or PTM mimics for protein function exploration.[16,29,34] However, as a powerful tool for peptide and protein multifunctionalization, more downstream applications of Dha modification need to be further explored. Reactions that can be controlled spatially and temporally are expected to expand downstream applications of the Dha modification methodology, but related reactions have yet to be developed.

To address these challenges and meet the growing needs of downstream applications, we turned our attention to the less explored 1,3-dipolar cycloaddition strategy. Although existing Dha modification strategies based on 1,3-dipolar cycloaddition have expanded the toolbox of methods available for peptide chemistry, they commonly require a long reaction time (12–72 hours) and harsh conditions (metal catalysts and/or organic solvents), thus preventing their general applicability.[18,20,33] Recently, a cycloaddition strategy for protein modification using nitrile oxides as 1,3-dipoles to react with Dha has been reported, enabling rapid modification of protein substrates in two hours.[35] However, nitrile oxides are prone to undergo side reactions with nucleophilic amino acids such as lysine, lacking chemical specificity for Dha. In our search for potentially more reactive and chemoselective 1,3-dipoles towards Dha residues, nitrile imines generated by photoactivation of tetrazoles attracted our attention.[36,37] Considering the broad functional group tolerance of photoinduced 1,3-dipolar cycloadditions between tetrazoles and various electron-deficient alkenes, we speculated that Dha could similarly undergo a fast and catalyst-free cycloaddition with tetrazoles. Herein, we report a photo-initiated 1,3-dipolar cycloaddition between 2,5-diaryl tetrazoles and Dha residues (Fig. 1B). Tetrazoles are readily triggered by 302 nm UV light from a hand-held LED lamp to form nitrile imine dipoles (Scheme S1†), which undergo spontaneous and rapid [3 + 2] cycloadditions with the unsaturated double bond of Dha residues in peptides and proteins, resulting in the formation of fluorescent pyrazoline products under mild and catalyst-free conditions within minutes. In addition, activation by

a specific wavelength of light enables precise temporal and spatial control of the reactions. Furthermore, as a fluorogenic reaction, the intense fluorescence of the pyrazoline product can be applied for cell imaging, further expanding the biomedical application of Dha chemical modification.

Results and discussion

In our initial study, protected Dha (Boc-Dha-OMe) was employed as the substrate to investigate the reactivity of Dha with 2,5-diaryl tetrazole under photoirradiation with 302 nm UV light (Table 1). A reaction mixture containing 2-(4-methoxyphenyl)-5-phenyltetrazole (**1a**), Boc-Dha-OMe, and the solvent was irradiated with a hand-held 302 nm UV lamp at room temperature. Notably, this reaction was completed within 10 minutes, as monitored *via* thin-layer chromatography (TLC), generating pyrazoline product **2a** with bright green fluorescence (as shown in Fig. S1†) in high isolated yields (74–80%). The time-course analysis demonstrated that the reactions were completed within 5–7 minutes (Fig. S2†). Further experiments showed the reaction's excellent solvent tolerance and rapid, efficient performance across a range of solvents, with particularly high efficiency in protic solvents including H_2O (Table 1, entries 1–6).

We next validated the reactivity of this reaction on Dha-containing peptides (Fig. 2). Cysteine-containing peptides **3a–e** were synthesized and then treated with methyl 2,5-dibromopentanoate (MeDBP) to generate Dha-containing peptides **4a–e** *via* bisalkylation-elimination. We initially utilized a C-terminal

---

Table 1 Light-initiated 1,3-dipolar cycloaddition between Boc-Dha-OMe and tetrazoles **1a/1b** in various solvents

Entry	Tetrazole	Substrate concentration (mM)		Solvent	Yield[a]
		Boc-Dha-OMe	Tetrazole		
1	**1a**	2.5	4.0	EtOAc	74.1%
2	**1a**	2.5	4.0	CH_2Cl_2	75.8%
3	**1a**	2.5	3.0	MeOH	78.0%
4	**1a**	2.5	3.0	MeCN	79.3%
5	**1a**	2.5	3.0	$MeCN : H_2O$ 3 : 1	78.2%
6	**1a**	1	1.2	H_2O	75.3%
7	**1b**	2.5	3.0	$MeCN : H_2O$ 3 : 1	77.1%
8	**1b**	1	1.2	$H_2O : MeCN$ 9 : 1	69.2%

[a] Isolated yields are reported.

---

amide-protected peptide **4a** as a model to react with tetrazole **1a** in the MeCN–H_2O mixed solvent. Under the same reaction conditions as those of the small-molecule substrates, the anticipated pyrazoline-modified product **5a** was obtained as the only product, yet its conversion rate of 63.2% required further improvement. By optimizing the stoichiometric ratio of the reaction and performing a stepwise addition of tetrazole **1a**, the conversion rate of peptide **4a** was increased to 87.0% (Fig. 2A, Scheme S5†). Under similar optimized conditions, we were delighted to find out that all the modifications of peptides **4b–e** with tetrazole **1a** were completed within 10–15 minutes, generating pyrazoline-modified peptides with bright green fluorescence in excellent conversion rates (83–98%) and isolated yields (68–84%) without any side-product formation (Fig. 2A, Scheme S5†). These results indicated that tetrazoles could chemoselectively react with Dha moieties in both C-terminal protected (**4a** and **4b**) and unprotected peptides (**4c–e**), and the reaction exhibited excellent compatibility with all natural amino acids. To further expand the scope of tetrazole reagents for downstream multifunctionalization, tetrazole **1b** bearing an alkynyl group was synthesized. After confirming its reactivity with the small molecule Dha substrate (Table 1, entries 7 and 8), we further reacted **1b** with peptides **4a–e** to obtain modified peptides with alkyne "reaction handles" (**6a–e**) (Fig. 2B, Scheme S6†), which exhibited bright blue fluorescence.

Inspired by the high yields and excellent tolerance to all natural amino acids, we aimed to extend this reaction to late-stage modifications of highly complex natural products. As a natural, complex and highly potent antibiotic against a broad range of Gram-positive bacteria,[38] thiostrepton has piqued our interest. Its complexity was partly exemplified by the presence of three Dha residues (Dha3, Dha16, and Dha17), one dehydrothreonine residue (Dhb8), four thiazoles, one thiazoline, three isolated hydroxyl groups, a diol, an amine, an imine, and a highly substituted pyridine (Fig. 3A).[39] Complex functional groups and multiple reaction sites bring great challenges to the site-selective Dha modification of thiostrepton. To date, only a limited number of late-stage modification strategies have been reported.[19,23,39–42] Although exhibiting predominant selectivity towards Dha16 or Dha17, which are located in the solvent-exposed tail region of thiostrepton, existing reactions have been observed to yield mixtures of heterogeneous modifications, generally including Dha16-modified products, Dha17-modified products, and doubly site-labelled products. Additionally, these reactions require hours to days to complete. The development of a rapid and site-specific Dha modification strategy for thiostrepton remains an outstanding challenge.

We aimed to investigate whether tetrazole reagents could tackle the aforementioned challenge. Our study started with the verification of the reactivity of tetrazole **1a** with thiostrepton (Scheme S7†). After stirring the reaction under 302 nm light for 15 minutes under the optimized reaction conditions, thiostrepton derivative **7a** with single-site pyrazoline modification was obtained, as characterized *via* reversed-phase high performance liquid chromatography (RP-HPLC), mass spectrometry (MS) and nuclear magnetic resonance (NMR) (Fig. S24, S27 and

Fig. 2 1,3-Dipolar cycloaddition reactions of Dha peptides **4a–e** with tetrazoles (A) **1a** and (B) **1b**. All peptide substrates **4a–e** were at a concentration of 1 mM. [a]Conversions were estimated *via* RP-HPLC. [b]Isolated yields of pyrazoline-modified products.

S28†). To our knowledge, this is currently the fastest Dha-based modification reaction for thiostrepton.

Next, we aspired to extend the reaction into a versatile, multifunctional derivatization strategy for thiostrepton. With this objective, we conducted the reaction between thiostrepton and tetrazole **1b** to install an alkynyl handle for further multifunctionalization (Fig. 3B, Scheme S7†). During RP-HPLC analysis of the reaction mixture, the optimized reaction conditions produced a clean reaction profile, with only product **7b** detected (Fig. 3C). After purification *via* RP-HPLC, **7b** was also characterized *via* MS as a single-site pyrazoline-modified product (Fig. S24 and S29†). Furthermore, an absolute preference for modification at Dha16 was confirmed *via* the combined analyses of 1D and 2D NMR spectra of the thiostrepton substrate and modified product **7b** (Fig. 3D–F). Initially, we referred to previous studies[19,23,42] to confirm the chemical shifts of the ^{1}H and ^{13}C signals from Dha3, Dha16, Dha17, and Dhb8 in the thiostrepton substrate (as shown in Fig. 3D–F (top)). Subsequently, by comparing the ^{1}H NMR spectra of **7b** (bottom) and thiostrepton (top) in Fig. 3D, we found that there were no C(sp²)–H NMR signals of the Dha16 side chain in the remaining Dha residues of product **7b**. Additionally, neither the [1]H–[1]H

correlated spectroscopy (COSY) spectra (Fig. 3E) nor the [1]H–[13]C heteronuclear multiple bond correlation (HMBC) spectra (Fig. 3F) of **7b** showed any NMR signals of Dha16, whereas the 1D and 2D NMR signals of Dha3, Dha17, and Dhb8 were all detected. These results indicated that the modification reaction occurred precisely at Dha16. We speculate that the site-selectivity for modification at Dha16 can be explained by the fact that this residue is the most electron-deficient site due to the presence of adjacent thiazole15 and Dha17, both of which are electron-withdrawing moieties.[19] In addition, previous studies have indicated that the highest occupied molecular orbital (HOMO) of a nitrile imine dipole generated by the photoactivation of tetrazole undergoes electron transfer with the lowest unoccupied molecular orbital (LUMO) of the alkene dipolarophile, leading to the occurrence of a [3 + 2] cycloaddition reaction.[43] The α,β-unsaturated double bond of Dha16 is adjacent to these two electron-withdrawing moieties, which lowers its LUMO energy and facilitates better alignment with the HOMO energy level of the nitrile imine. Therefore, the cycloaddition reaction exhibits a significant preference for modification at Dha16, even demonstrating explicit site-specificity.
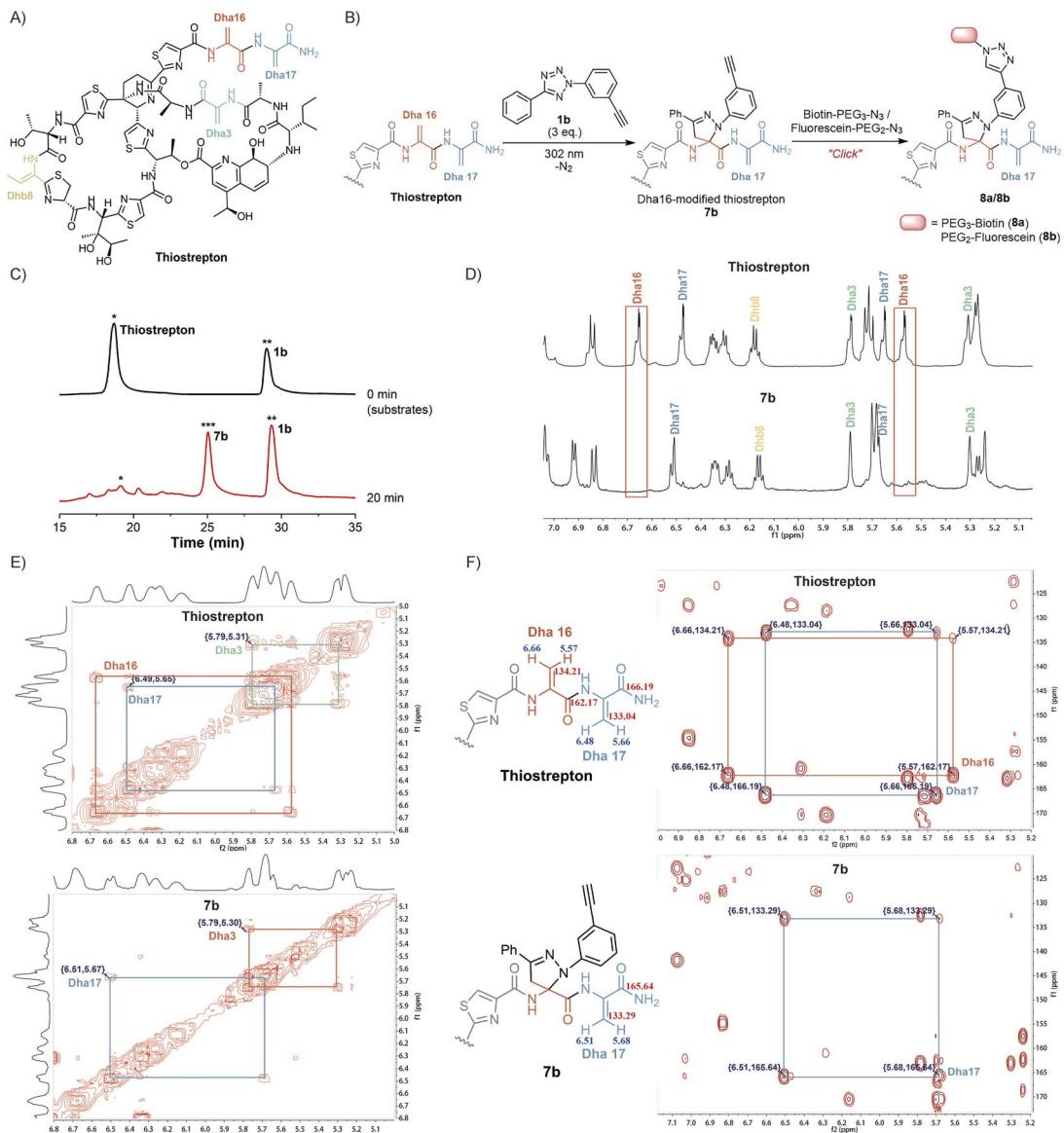
Fig. 3 Site-selective labelling of thiostrepton *via* light-initiated 1,3-dipolar cycloaddition of Dha and tetrazole **1b**. (A) Chemical structure of thiostrepton. (B) Two-step reaction for site-specific labelling of Dha16 on thiostrepton. (C) HPLC analysis of the reaction mixture of thiostrepton and tetrazole **1b** at 0 min (top) and 20 min (bottom). (D) ^{1}H NMR spectra of thiostrepton and Dha16-labelled product **7b**. Chemical shifts of signals from the C(sp^2)−H of Dha3, Dha16, Dha17, and Dhb8 are assigned. (E) 2D-NMR spectra (^{1}H−^{1}H COSY) of thiostrepton and **7b**, which show ^{1}H−^{1}H couplings in Dha16 and Dha17. (F) 2D-NMR spectra (^{1}H−^{13}C HMBC) of thiostrepton and **7b**. Long range ^{1}H−^{13}C couplings *via* a H−C−C−C path are measured and assigned.

In addition, the installation of an alkynyl group on thiostrepton enabled downstream functionalization through click reactions with various commercially available azide reagents. Herein, the reactions of biotin-PEG$_3$-azide and fluorescein-PEG$_2$-azide with **7b** were utilized as examples to illustrate the feasibility and great potential of this reaction for the multi-functionalization of highly complex natural products (Fig. 3B). Under mild conditions, biotinylated thiostrepton derivative **8a** and fluorescein-labelled product **8b** were obtained with isolated yields of 61.2% and 52.7%, respectively (Scheme S8†). This reaction simplified the late-stage chemical modification of thiostrepton, allowing for more efficient and rapid site-specific

modification of Dha16 under milder conditions without catalysts or additives. Compared to previous methods that needed hours or even days under metal catalysis, our method enabled the efficient synthesis of more novel analogues of homogeneous thiostrepton derivatives.

With the goal of investigating the applicability of this method to other biologically relevant molecules containing Dha motifs, we applied this reaction for Dha-containing protein modification (Fig. 4). To investigate the reactivity towards proteins containing a Dha residue, we selected alpha-synuclein (α-syn) as a model. Considering the lack of cysteine residues in the natural sequence of wild-type α-syn, we mutated Ser129 to
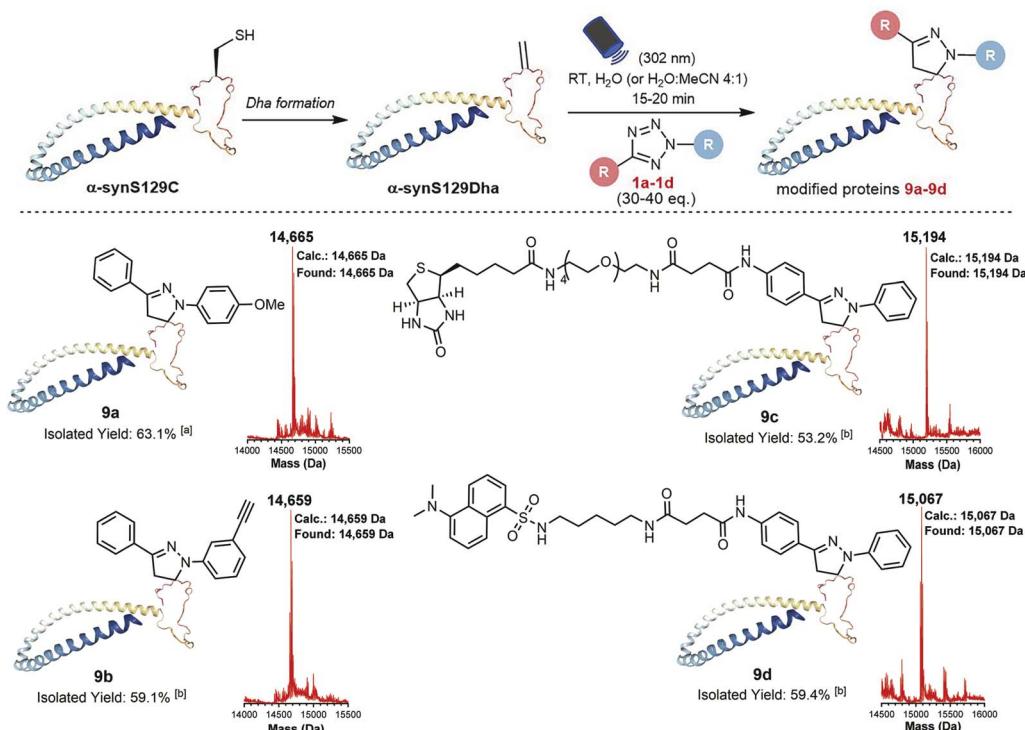
Fig. 4 Chemoselective labelling of the α-synS129Dha protein *via* light-initiated 1,3-dipolar cycloaddition between Dha and tetrazoles **1a–d**. The concentration of α-synS129Dha was 34.6 μM (0.5 mg mL^{-1}) in each reaction. [a]The reaction was performed in H_2O. [b]The reactions were conducted in the H_2O–MeCN mixed solvent (4 : 1, v/v).

Cys129 and further converted it to Dha to create a potential reaction site, obtaining the α-synS129Dha variant. Initially, we modified α-synS129Dha with tetrazole **1a** under conditions similar to those of peptide modification. The initial stoichiometric ratio of **1a** to α-synS129Dha was set at 10 : 1. After stirring for 30 minutes under irradiation with 302 nm UV light, the reaction mixture was analysed *via* RP-HPLC and MS. However, the expected product was not obtained. By optimizing the stoichiometric ratio of **1a** to α-synS129Dha at 30 : 1 and irradiating the reaction mixture with 302 nm UV light for 15 minutes, we obtained the pyrazoline-modified protein **9a** in H_2O with a yield of 63.1%. Through CD spectroscopy analysis of wild-type α-syn, α-synS129Dha and pyrazoline-modified protein **9a**, we have confirmed that this chemical modification did not cause any disruption to the protein's secondary and tertiary structures (Fig. S38, Table S1†). Then we proceeded to expand the scope of tetrazoles. We synthesized tetrazole **1c** labelled with biotin and tetrazole **1d** labelled with fluorescent dansylcadaverine for straightforward one-step protein labelling. As shown in Fig. 4, α-synS129Dha could be efficiently and rapidly functionalized with tetrazoles **1a–d**, resulting in the generation of **9a–d** in moderate to high yields (53–63%) in H_2O or aqueous solution containing 20% MeCN (Fig. 4).

The exceptional efficacy of this reaction in modifying peptides and proteins in solution prompts the broadening of its potential biological applications. The fast rate, high efficiency, mild conditions and simplicity of the reactions between Dha and tetrazoles make them highly promising for cell labeling.

Furthermore, the fluorogenic properties of this reaction enables *in situ* imaging of cells without using additional fluorophores. Notably, the fluorescence generated *in situ* facilitates direct monitoring of the reaction progress to determine the effectiveness of cell labelling. Moreover, the photocontrollability of this reaction provides potential advantages in terms of time and space control. Therefore, we investigated the feasibility of *in situ* imaging of B16-OVA mouse melanoma cells using a light-triggered reaction between tetrazoles and cyclic RGD peptides (Fig. 5A). RGD peptides refer to a series of short peptides containing an arginine-glycine-aspartic acid sequence, which specifically bind to integrins that are overexpressed in tumour cells.[44,45] Currently, there have been extensive studies on tumour cell-targeted imaging and cancer-targeted drug delivery based on the specific binding of linear RGD peptides or cyclic RGD peptides with integrin α$_v$β$_3$.[44–49] In our study, we chose cyclo(RGDfC) as a sensitive integrin α$_v$β$_3$ receptor ligand[50,51] and treated it with MeDBP to generate cyclo(RGDfDha) (**10**) *via* a bisalkylation–elimination reaction (Scheme S9†). Initially, we tested the reactions between tetrazoles (**1a** and **1b**) and cyclic RGD peptide **10** in solution and successfully obtained modified cyclic peptides **11a** with bright green fluorescence and **11b** with bright blue fluorescence. The fluorescence excitation and emission spectra of both **11a** and **11b** were obtained *via* fluorescence spectral characterization (Fig. S43†).

Next, we aimed to achieve *in situ* imaging of B16-OVA tumour cells by targeting integrin receptors utilizing the reactions between tetrazoles and the Dha residue on cyclic peptide **10**
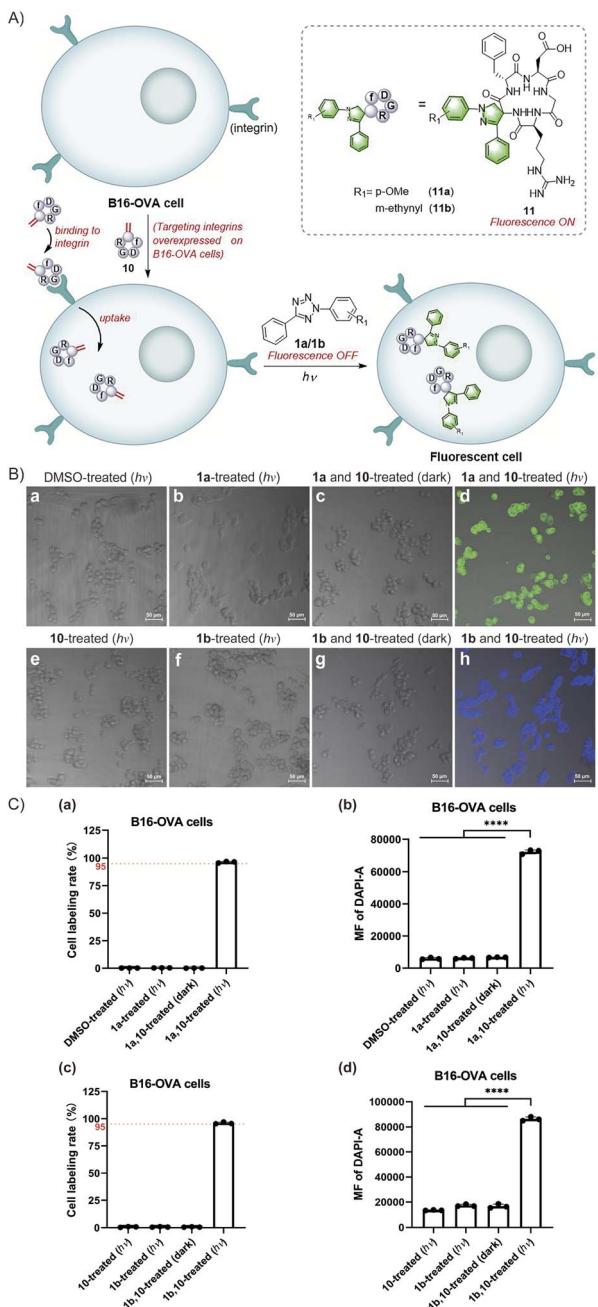
Fig. 5 *In situ* imaging of tumour cells using a cyclic RGD peptide. (A) Schematic illustration. (B) Merged images of DAPI and T-PMT channels of B16-OVA cells captured using a confocal laser scanning microscope. Scale bar = 50 μm. B16-OVA cells in (a)–(h) were sequentially treated with (a) 1% DMSO (*hν*), (b) 160 μM tetrazole **1a** (*hν*), (c) 160 μM **1a** and 80 μM cyclic peptide **10** (dark), (d) 160 μM **1a** and 80 μM **10** (*hν*), (e) 100 μM **10** (*hν*), (f) 200 μM tetrazole **1b** (*hν*), (g) 200 μM **1b** and 100 μM **10** (dark), and (h) 200 μM **1b** and 100 μM **10** (*hν*). Among them, cells in (a), (b), (d), (e), (f), and (h) were treated with 15-min photoirradiation at 302 nm. (C) Flow cytometry analysis of B16-OVA cells. Bar graphs in (a) and (c) represent the cell labelling rate for each population. Bar graphs in (b) and (d) represent the mean fluorescence (MF) of the DAPI channel for each population. The error bars indicate the standard deviations calculated from three independent experiments. Statistical significance was determined by one-way analysis of variance (*P* value: ****$P < 0.0001$).

(Fig. 5A). To begin, we evaluated the cytotoxicity of the reactants and products on B16-OVA cells using Cell Counting Kit-8 (CCK-8) and found no significant toxicity at various concentrations of tetrazoles **1a** and **1b**, cyclic peptide substrate **10**, and modified peptides **11a** and **11b** (Fig. S44†). Then, we incubated the cells with cyclo(RGDfDha) (**10**) for 12 hours to ensure full binding of the cyclic RGD peptide to integrin receptors and subsequent cellular uptake. After washing the cells with phosphate buffered saline (PBS) to remove excess cyclic peptide **10** in the culture medium, we added tetrazole **1a** or **1b** to the cells and incubated them for 30 minutes, followed by a 15-minute reaction under irradiation with a 302 nm hand-held UV lamp. The cellular fluorescence was recorded using a confocal laser scanning microscope equipped with a DAPI filter. As shown in Fig. 5B(d) and (h), strong fluorescent signals were detected and effectively colocalized with the cells, and nearly all cells in the field of view were successfully labelled. In contrast, cells incubated with **10** and a tetrazole reagent (**1a** or **1b**) without subsequent photo-irradiation did not show evident fluorescence [Fig. 5B(c) and (g)]. Moreover, no significant fluorescence signals were detected in cells treated separately with tetrazole **1a** and **1b** and cyclic peptide **10** followed by 15 minutes of UV-light irradiation [Fig. 5B(b), (e) and (f)]. After verifying the feasibility of this reaction for cell imaging, we aimed to accurately determine the fluorescent labelling ratios of B16-OVA cells. After undergoing the same reaction process as above, the cells were analysed by flow cytometry, utilizing a 355 nm violet laser for excitation and a 450/50 bandpass filter for fluorescence detection. As shown in Fig. 5C, B16-OVA cells showed a significant increase in the population of fluorescent cells after the photoinitiated reaction compared to B16-OVA cells treated with dimethyl sulfoxide (DMSO). We demonstrated that both **1a** and **1b** exhibited high reaction efficiency towards cyclic peptide **10**, which was able to fully bind to the integrin receptors on B16-OVA cells and undergo cellular uptake, resulting in high cellular fluorescence labelling rates of 95–100% [Fig. 5C(a) and (c)]. The bar graphs (b) and (d) in Fig. 5C indicated that the average fluorescence intensity (MF) of labelled cells was significantly enhanced compared to that of the relevant control groups. In contrast, the control groups using tetrazoles **1a** and **1b** and cyclic peptide **10** to incubate cells separately followed by 15-minute UV-light irradiation showed no fluorescent labelling. Similarly, cells treated with tetrazole and cyclic peptide **10** without UV-light irradiation remained unlabelled. These results were consistent with our observations *via* a confocal laser scanning microscope.

Conclusions

In summary, we developed a versatile method for the late-stage modification of various Dha-containing peptides and proteins using a photoinitiated 1,3-dipolar cycloaddition reaction between Dha and tetrazoles. This remarkable strategy introduces the first catalyst-free photoinitiated reaction into the existing toolbox of Dha chemical modification. During this process, we demonstrated the strategic advantages of this rapid, mild, highly selective, and photocontrollable methodology for

the chemical modification of conventional peptide substrates and complex natural product peptides containing Dha moieties. The addition of an alkyne as a reaction handle on the substrates enables diverse downstream functionalizations *via* azide–alkyne cycloaddition. Notably, this strategy has considerable potential for expanding to the late-stage modification of other complex natural product peptides containing Dha residues. It provides a powerful tool for further structural optimization and property exploration. Moreover, we have shown the significant efficacy of this cycloaddition reaction in protein modification by utilizing diverse tetrazole reagents in aqueous solution. Additionally, by exploiting the unique fluorescence generation properties of this reaction, we have expanded the biological applications beyond those explored by previous Dha modification strategies. We utilized the reaction between a Dha-containing cyclic RGD peptide and tetrazoles to achieve *in situ* imaging of B16-OVA cells, providing the first application of Dha modification strategies in live cell imaging.

Data availability

All experimental supporting data and procedures associated with this article have been provided in the ESI.†

Author contributions

M. Z. and Y. L. conceived the idea of the research. M. Z. performed all experiments and collected the experimental data with assistance from P. H. M. Z. analyzed the results and wrote the manuscript with the guidance of Y. L. and P. H. Y. L. revised the article and supervised the project. All authors contributed to the editing of the manuscript.

Conflicts of interest

There are no conflicts to declare.

References

1 E. A. Hoyt, P. M. S. D. Cal, B. L. Oliveira and G. J. L. Bernardes, *Nat. Rev. Chem*, 2019, **3**, 147–171.
2 N. Krall, F. P. da Cruz, O. Boutureira and G. J. L. Bernardes, *Nat. Chem.*, 2016, **8**, 102–112.
3 L. H. Jones, *RSC Chem. Biol.*, 2020, **1**, 298–304.
4 J.-J. Hu, P.-Y. He and Y.-M. Li, *J. Pept. Sci.*, 2021, **27**, e3286.
5 N. H. Fischer, M. T. Oliveira and F. Diness, *Biomater. Sci.*, 2023, **11**, 719–748.
6 D. Siodlak, *Amino Acids*, 2015, **47**, 1–17.

7 M. A. Ortega and W. A. van der Donk, *Cell Chem. Biol.*, 2016, **23**, 31–44.
8 H. Chen, Y. Zhang, Q.-Q. Li, Y.-F. Zhao, Y.-X. Chen and Y.-M. Li, *J. Org. Chem.*, 2018, **83**, 7528–7533.
9 A. A. Vinogradov, M. Nagano, Y. Goto and H. Suga, *J. Am. Chem. Soc.*, 2021, **143**, 13358–13369.
10 J. Dadova, S. R. G. Galan and B. G. Davis, *Curr. Opin. Chem. Biol.*, 2018, **46**, 71–81.
11 H. Li, H. Xu, Y. Zhou, J. Zhang, C. Long, S. Li, S. Chen, J.-M. Zhou and F. Shao, *Science*, 2007, **315**, 1000–1003.
12 J. M. Chalker, S. B. Gunnoo, O. Boutureira, S. C. Gerstberger, M. Fernandez-Gonzalez, G. J. L. Bernardes, L. Griffin, H. Hailu, C. J. Schofield and B. G. Davis, *Chem. Sci.*, 2011, **2**, 1666–1676.
13 J. W. Bogart and A. A. Bowers, *Org. Biomol. Chem.*, 2019, **17**, 3653–3669.
14 M. Q. Zhang, P. Y. He and Y. M. Li, *Chem. Res. Chin. Univ.*, 2021, **37**, 1044–1054.
15 A. M. Freedy, M. J. Matos, O. Boutureira, F. Corzana, A. Guerreiro, P. Akkapeddi, V. J. Somovilla, T. Rodrigues, K. Nicholls, B. Xie, G. Jimenez-Oses, K. M. Brindle, A. A. Neves and G. J. L. Bernardes, *J. Am. Chem. Soc.*, 2017, **139**, 18365–18375.
16 A. Yang, S. Ha, J. Ahn, R. Kim, S. Kim, Y. Lee, J. Kim, D. Soell, H.-Y. Lee and H.-S. Park, *Science*, 2016, **354**, 623–626.
17 T. H. Wright, B. J. Bower, J. M. Chalker, G. J. L. Bernardes, R. Wiewiora, W.-L. Ng, R. Raj, S. Faulkner, M. R. J. Vallee, A. Phanumartwiwath, O. D. Coleman, M.-L. Thezenas, M. Khan, S. R. G. Galan, L. Lercher, M. W. Schombs, S. Gerstberger, M. E. Palm-Espling, A. J. Baldwin, B. M. Kessler, T. D. W. Claridge, S. Mohammed and B. G. Davis, *Science*, 2016, **354**, 597.
18 G. J. Bao, P. Wang, G. F. Li, C. J. Yu, Y. P. Li, Y. Y. Liu, Z. Y. He, T. T. Zhao, J. Rao, J. Q. Xie, L. Hong, W. S. Sun and R. Wang, *Angew. Chem., Int. Ed.*, 2021, **60**, 5331–5338.
19 R. H. de Vries, J. H. Viel, R. Oudshoorn, O. P. Kuipers and G. Roelfes, *Chem. –Eur. J.*, 2019, **25**, 12698–12702.
20 L. M. Repka, J. Ni and S. E. Reisman, *J. Am. Chem. Soc.*, 2010, **132**, 14418–14420.
21 S. R. G. Galan, J. R. Wickens, J. Dadova, W.-L. Ng, X. Zhang, R. A. Simion, R. Quinlan, E. Pires, R. S. Paton, S. Caddick, V. Chudasama and B. G. Davis, *Nat. Chem. Biol.*, 2018, **14**, 955–963.
22 P.-Y. He, H. Chen, H.-G. Hu, J.-J. Hu, Y.-J. Lim and Y.-M. Li, *Chem. Commun.*, 2020, **56**, 12632–12635.
23 R. H. de Vries, J. H. Viel, O. P. Kuipers and G. Roelfes, *Angew. Chem., Int. Ed.*, 2021, **60**, 3946–3950.
24 H. K. Jiang, P. Kurkute, C. L. Li, Y. H. Wang, P. J. Chen, S. Y. Lin and Y. S. Wang, *Biochemistry*, 2020, **59**, 3796–3801.
25 K. C. Tang, S. M. Maddox, K. M. Backus and M. Raj, *Chem. Sci.*, 2022, **13**, 763–774.
26 J.-A. Shin, J. Kim, H. Lee, S. Ha and H.-Y. Lee, *J. Org. Chem.*, 2019, **84**, 4558–4565.
27 T. Rossolini, B. Ferko and D. J. Dixon, *Org. Lett.*, 2019, **21**, 6668–6673.
28 A. A. Shah, M. J. Kelly and J. J. Perkins, *Org. Lett.*, 2020, **22**, 2196–2200.

29 B. Josephson, C. Fehl, P. G. Isenegger, S. Nadal, T. H. Wright, A. W. J. Poh, B. J. Bower, A. M. Giltrap, L. Chen, C. Batchelor-McAuley, G. Roper, O. Arisa, J. B. I. Sap, A. Kawamura, A. J. Baldwin, S. Mohammed, R. G. Compton, V. Gouverneur and B. G. Davis, *Nature*, 2020, **585**, 530–537.

30 R. C. W. van Lier, A. D. de Bruijn and G. Roelfes, *Chem. –Eur. J.*, 2021, **27**, 1430–1437.

31 X. X. Qi, S. Jambu, Y. N. Ji, K. M. Belyk, N. R. Panigrahi, P. S. Arora, N. A. Strotman and T. N. Diao, *Angew. Chem., Int. Ed.*, 2022, **61**, e20221331.

32 X. Peng, K. Xu, Q. Zhang, L. Liu and J. Tan, *Trends Chem.*, 2022, **4**, 643–657.

33 M. R. Aronoff, B. Gold and R. T. Raines, *Org. Lett.*, 2016, **18**, 1538–1541.

34 J. Dadová, K.-J. Wu, P. G. Isenegger, J. C. Errey, G. J. L. Bernardes, J. M. Chalker, L. Raich, C. Rovira and B. G. Davis, *ACS Cent. Sci.*, 2017, **3**, 1168–1173.

35 A. Phanumartwiwath, C. Kesornpun, D. Chokchaichamnankit, A. Khongmanee, P. Diskul-Na-Ayudthaya, T. Ruangjaroon, C. Srisomsap, P. Kittakoop, J. Svasti and S. Ruchirawat, *Chembiochem*, 2023, e202300268.

36 J. S. Clovis, A. Eckell, R. Huisgen and R. Sustmann, *Chem. Ber.*, 1967, **100**, 60–70.

37 Y. Z. Wang, C. I. R. Vera and Q. Lin, *Org. Lett.*, 2007, **9**, 4155–4158.

38 X. Just-Baringo, F. Albericio and M. Alvarez, *Mar. Drugs*, 2014, **12**, 317–351.

39 H. M. Key and S. J. Miller, *J. Am. Chem. Soc.*, 2017, **139**, 15460–15466.

40 R. J. Scamp, E. DeRamon, E. K. Paulson, S. J. Miller and J. A. Ellman, *Angew. Chem., Int. Ed.*, 2020, **59**, 890–895.

41 T. Brandhofer and O. G. Mancheno, *ChemCatChem*, 2019, **11**, 3797–3801.

42 R. H. de Vries and G. Roelfes, *Chem. Commun.*, 2020, **56**, 11058–11061.

43 R. K. V. Lim and Q. Lin, *Acc. Chem. Res.*, 2011, **44**, 828–839.

44 F. Danhier, A. Le Breton and V. Preat, *Mol. Pharm.*, 2012, **9**, 2961–2973.

45 M. Nieberler, U. Reuning, F. Reichart, J. Notni, H. J. Wester, M. Schwaiger, M. Weinmuller, A. Rader, K. Steiger and H. Kessler, *Cancers*, 2017, **9**, 116.

46 K. N. Sugahara, T. Teesalu, P. P. Karmali, V. R. Kotamraju, L. Agemy, D. R. Greenwald and E. Ruoslahti, *Science*, 2010, **328**, 1031–1035.

47 Y. J. Chen, L. X. Jia, G. L. Zhu, W. Wang, M. Geng, H. X. Lu, Y. Zhang, M. H. Zhou, F. Y. Zhang and X. Z. Cheng, *Bioorganic Med. Chem. Lett.*, 2022, **73**, 128888.

48 S. Asati, V. Pandey and V. Soni, *Int. J. Pept. Res. Ther.*, 2019, **25**, 49–65.

49 M. D. Wang, G. T. Lv, H. W. An, N. Y. Zhang and H. Wang, *Angew. Chem., Int. Ed.*, 2022, **61**, e20211364.

50 R. Hennig, S. Kuespert, A. Haunberger, A. Goepferich and R. Fuchshofer, *J. Drug Targeting*, 2016, **24**, 952–959.

51 N. Raval, H. Jogi, P. Gondaliya, K. Kalia and R. K. Tekade, *Mol. Pharm.*, 2021, **18**, 641–666.